

Theory of Cooling of Room Temperature Benzene upon Photo-Excitation to the S₁ State

Yong He and Eli Pollak*

Chemical Physics Department, Weizmann Institute of Science, 76100, Rehovot, Israel

Received: October 31, 2000; In Final Form: August 7, 2001

An ab initio harmonic study is presented for the nascent vibrational energy distribution of room-temperature benzene when photoexcited to the S₁ state. The dependence on photoexcitation frequency and pulse width is investigated. We find, that even though the transition is symmetry disallowed, the Herzberg–Teller mechanism by which the nuclear motion induces the transition, can lead to cooling of the molecule at the transition frequencies corresponding to a mode of E_{2g} symmetry. The extent of cooling decreases with increasing pulse width, but even with a pulse width of 90 cm⁻¹ one still finds significant cooling of the vibrational population. Cooling is also found for deuterated benzene. The energy deposited in the molecule is found to be very sensitive to the excitation frequency, provided that the pulse width is sufficiently narrow.

I. Introduction

Excitation of a room temperature polyatomic molecule is usually accompanied by heating or cooling of the nascent vibrational distribution. The cooling phenomenon was first suggested by Beddard et al.¹ in their studies of the pressure dependence of fluorescence decay rates of naphthalene. It was also used recently by Gershinsky and Pollak² to explain the rather large differences between fluorescence decay rates of stilbene in the gas and liquid phases. Within the Condon approximation, they found that typically, if the excitation wavelength is to the blue of the transition frequency from the ground vibrational state of the ground electronic state, to the ground vibrational state in the excited electronic state (ω_{00}), then the molecule is heated. Interestingly, at the ω_{00} transition frequency or somewhat to the red of it one may expect under rather general conditions³ that the nascent distribution will be cooled. The cooling effect is predicted to be generic for polyatomic molecules³ and is caused by the lowering of vibrational frequencies in the excited electronic surface (in general, this lowering reflects the weakening of the chemical bonds due to the excitation of the electron).

Thus far though, the cooling phenomenon has not been studied for molecules for which the Condon approximation, in which the dipole moment is taken to be a constant, is not valid due to symmetry considerations. Also, the studies of the Stilbene molecule were limited to model potentials which were not based on ab initio computations. Both of these limitations are remedied in this paper, in which we study the nature of the nascent vibrational population in the excited S₁ state of the benzene molecule and its isotopic derivative C₆D₆.

The harmonic theory for the absorption spectrum, the nascent vibrational energy distribution in the excited state and its moments, is presented in Section II. In Section III, we describe the harmonic model for the ground and excited-state normal modes and position shifts for the benzene molecule, based on the ab initio force field of ref 4. The thermal absorption spectrum and the dependence of the nascent vibrational energy distribution in the excited state on the excitation frequency are presented in Section IV for benzene and deuterated benzene. The thermal absorption spectrum is in agreement with the experimental spectrum. Due to the fact that the density of states of benzene is not very large, we find that the average energy in the excited

state is rather sensitive to the excitation wavelength and to the temporal shape of the excitation pulse. Cooling is found, both to the red and the blue of the ω_{00} transition frequency. The extent of cooling is reduced as the pulse duration gets shorter, but this is compensated by a broader range of excitation frequencies that lead to cooling. For room-temperature ground electronic state benzene, the maximal cooling leads to an excited state “temperature” of 73 K. We end in Section V with a discussion of these results and the implications for other systems such as naphthalene and stilbene.

II. Theory For The Spectrum, Energy Moments And Distribution

A. General Expressions. We assume that the ground and excited electronic states of the polyatomic molecule are described by the Hamiltonians H_g and H_e , respectively. The respective vibrational eigenfunctions and eigenvalues are denoted as $|g_i\rangle$ and E_{g_i} for the ground-state Hamiltonian and $|e_j\rangle$ and E_{e_j} for the excited-state Hamiltonian. The absorption spectrum $F(\omega, \Delta\omega, \beta)$ for excitation with a Gaussian pulse whose average frequency is ω and whose width is $\Delta\omega$, may be written down formally as

$$F(\omega, \Delta\omega, \beta) = \frac{1}{Z(\beta)\sqrt{2\pi\Delta\omega^2}} \int_{-\infty}^{\infty} d\omega' e^{-(\omega' - \omega)^2/(2\Delta\omega^2)} \times \sum_{i,j} | \langle e_j | \mu | g_i \rangle |^2 e^{-\beta E_{g_i}} \delta(\Delta E + E_{e_j} - E_{g_i} - \hbar\omega') \quad (2.1)$$

where ΔE is the energy difference between the bottom of the ground and excited-state potentials; $\beta = 1/k_B T$ is the inverse temperature of the molecule in the ground state, $Z(\beta) \equiv \sum_i e^{-\beta E_{g_i}}$ is the partition function for the molecules in the ground state and μ is the dipole operator.

Using the Fourier representation of the Dirac delta function, the absorption spectrum can be re-expressed as a Fourier transform

$$F(\omega, \Delta\omega, \beta) = \frac{1}{2\pi\hbar Z(\beta)} \int_{-\infty}^{+\infty} dt e^{-it/(\Delta E - \hbar\omega)\hbar} e^{-t^2\Delta\omega^2/2} \chi(t, \beta) \equiv \frac{Z(\omega, \Delta\omega, \beta)}{Z(\beta)} \quad (2.2)$$

where the correlation function $\chi(t, \beta)$ is defined as

$$\chi(t, \beta) = \text{Tr} [\mu e^{-itH_e/\hbar} \mu e^{-(\beta - it/\hbar)H_g}] \quad (2.3)$$

The average energy in the excited state is given by²

$$\langle E \rangle(\omega, \Delta\omega, \beta) = \hbar\omega - \Delta E - \left(\frac{\partial}{\partial\beta} - \frac{\hbar\Delta\omega^2}{2} \frac{\partial}{\partial\omega} \right) \log(Z(\omega, \Delta\omega, \beta)) \quad (2.4)$$

All higher moments of the energy in the excited state are derived from the recursion relation³

$$\langle E^n \rangle(\omega, \Delta\omega, \beta) = \left(\hbar\omega - \Delta E - \frac{\partial}{\partial\beta} + \frac{\hbar\Delta\omega^2}{2} \frac{\partial}{\partial\omega} \right) \langle E^{n-1} \rangle(\omega, \Delta\omega, \beta) \quad (2.5)$$

The energy distribution³ $P_e(E; \omega, \beta)$ may be evaluated from the following formulas

$$P_e(E; \omega, \Delta\omega, \beta) = \frac{1}{(2\pi)^2 \hbar Z(\omega, \Delta\omega, \beta)} \int_{-\infty}^{+\infty} dt \int_{-\infty}^{\infty} dt' \times e^{-it(\Delta E - \hbar\omega)/\hbar} e^{-t^2\Delta\omega^2/2} e^{it'E/\hbar} \chi_e(t, t'; \beta) \quad (2.6)$$

where the two point correlation function $\chi_e(t, t'; \beta)$ is

$$\chi_e(t, t'; \beta) = \text{Tr} \mu e^{-i(t+t')H_e/\hbar} \mu e^{-(\beta - it/\hbar)H_g} \quad (2.7)$$

B. Specification to the Harmonic Model. To apply the theory to the benzene molecule we will use a harmonic force field for the ground and excited states. Because Duschinskii⁵ rotations for benzene may be neglected,⁶ it is sufficient to take the Hamiltonians as

$$H_g = \frac{1}{2} \sum_{i=1}^N (p_i^2 + \omega_{g_i}^2 q_i^2) \quad (2.8)$$

$$H_e = \frac{1}{2} \sum_{i=1}^N [p_i^2 + \omega_{e_i}^2 (q_i - q_{i_0})^2] \quad (2.9)$$

where q_i, p_i are the i -th mass weighted normal mode coordinate and momentum, respectively. In this model, the frequency and the equilibrium position in the excited state are shifted with respect to the ground state.

The dipole operator will be taken to lowest order only as

$$\mu = \sum_{j=1}^M \mu_j q_j \quad (2.10)$$

where the sum is over M modes, usually much less than the total number of normal modes N because many transitions are disallowed by symmetry. It is then a matter of algebra⁷ to show that the correlation function is a product of single mode

correlation functions. The single mode correlation function obtained if $\mu = I$ is

$$\chi_{j0}(t, \beta) = \left[\frac{a_{gj} a_{ej}}{(b_{gj} + b_{ej})^2 - (a_{gj} + a_{ej})^2} \right]^{1/2} \times e^{i g_{j0}^2 (b_{gj} - a_{gj})(b_{ej} - a_{ej}) / [(b_{ej} - a_{ej} + b_{gj} - a_{gj}) \hbar]} \quad (2.11)$$

Here, the a 's and b 's are and

$$a_{gj} = \frac{\omega_{g_j}}{\sin(\hbar\omega_{g_j} t_c)} \quad (2.12)$$

$$b_{gj} = \frac{\omega_{g_j}}{\tan(\hbar\omega_{g_j} t_c)} \quad (2.13)$$

$$a_{ej} = \frac{\omega_{e_j}}{\sin(\hbar\omega_{e_j} t)} \quad (2.14)$$

$$b_{ej} = \frac{\omega_{e_j}}{\tan(\hbar\omega_{e_j} t)} \quad (2.15)$$

$$t_c = -i\beta - t. \quad (2.16)$$

The correlation function is then found to be

$$\chi(t, \beta) = \prod_{j=1}^N \chi_{j0}(t, \beta) \times \left(\sum_{i,l=1}^M \mu_j \mu_l q_{j0} q_{l0} \frac{(b_{ej} - a_{ej})(b_{el} - a_{el})}{(b_{ej} + b_{gj} - a_{gj} - a_{ej})(b_{el} + b_{gl} - a_{gl} - a_{el})} + i\hbar \sum_{j=1}^M \mu_j^2 \frac{a_{ej} + a_{gj}}{(b_{ej} + b_{gj})^2 - (a_{gj} + a_{ej})^2} \right). \quad (2.17)$$

This is the central expression of this subsection. Given the dipole transition strengths of the normal modes (μ_j) and their frequencies and shifts, it is relatively straightforward to compute the correlation function and from it the thermal absorption spectrum and the moments of the energy in the excited electronic state. The two point correlation function (eq 2.7) has the same form as in eq 2.17, except that the time variable t is to be replaced by $t + t'$, whereas t_c remains as before.

III. Ab Initio Harmonic Model For Benzene

The harmonic force fields have been calculated for the ground state (S_0), and the first excited singlet state (S_1) of benzene by Pulay et al.⁸ and by Swiderek et al.⁴ In our computations, we have used the force fields of Swiderek et al. to compute the vibrational frequencies and the position shifts of benzene in both states. Benzene (C_6H_6) possesses $N = 30$ normal modes. Due to the D_{6h} point group of benzene, there are only 20 different vibrational frequencies, of these, 10 belong to degenerate normal modes.

The molecular geometry and the force fields obtained from the ab initio calculations are represented in internal coordinates.

TABLE 1: Normal Mode Frequencies, Shifts, and Dipole Transition Moments of Ground (S_0) and Excited (S_1) Benzene and Deuterated Benzene

symm	C_6H_6					C_6D_6				
	ω_g^a	ω_e^a	$\omega_e - \omega_g^a$	\tilde{q}_0^b	μ^c	ω_g	ω_e	$\omega_e - \omega_g^a$	\tilde{q}_0^b	
a_{1g}	3187	3204	17	0.415	0.000	2365	2373	8	1.292	
	979	902	-77	1.710	0.00	933	861	-72	1.633	
a_{2g}	1353	1323	-30	0.000	0.000	1050	1025	-25	0.000	
	3155	3174	19	0.000	0.065	2327	2339	12	0.000	
e_{2g}	1611	1560	-51	0.000	0.257	1574	1523	-51	0.000	
	1173	1151	-22	0.000	0.088	857	838	-19	0.000	
	592	529	-63	0.000	0.217	555	499	-56	0.000	
b_{1u}	3145	3165	20	0.000	0.000	2316	2331	15	0.000	
	998	963	-35	0.000	0.000	958	924	-34	0.000	
b_{2u}	1342	1739	397	0.000	0.000	1334	1739	405	0.000	
	1163	1149	-14	0.000	0.000	827	812	-15	0.000	
e_{1u}	3173	3189	16	0.000	0.000	2349	2354	5	0.000	
	1479	1400	-79	0.000	0.000	1343	1221	-122	0.000	
	1023	916	-107	0.000	0.000	773	723	-50	0.000	
b_{2g}	916	641	-275	0.000	0.000	754	536	-218	0.000	
	650	434	-216	0.000	0.000	559	366	-193	0.000	
e_{1g}	781	548	-233	0.000	0.000	607	425	-182	0.000	
a_{2u}	631	480	-151	0.000	0.000	463	352	-111	0.000	
e_{2u}	891	628	-263	0.000	0.000	721	505	-216	0.000	
	383	262	-121	0.000	0.000	334	229	-105	0.000	

^a Frequencies are given in units of cm^{-1} . ^b Position shifts are dimensionless and defined as $\tilde{q}_0 = q_0 \sqrt{\omega_e/\hbar}$. ^c Dipole transition moments are dimensionless, taken from ref 15.

The transformation from internal coordinates to normal coordinates is

$$q_i = \sum_{j=1}^N L_{ij}^{-1} s_j \quad (3.1)$$

where s_j represents the j -th internal coordinate. The inverse transformation is therefore

$$s_j = \sum_{i=1}^N L_{ji} q_i \quad (3.2)$$

where the L_{ji} 's are the coefficients of the inverse transformation of the L^{-1} matrix. To get the transformation coefficients L_{ij}^{-1} , we have to reconstruct (using the notation of Wilson, Decius, and Cross⁹) the \mathbf{F} and \mathbf{G} matrixes. We then diagonalize the matrix \mathbf{GF} by a method due to Miyazawa¹⁰. The calculated vibrational frequencies and position shifts of the S_0 and S_1 states are given in Table 1.

In the single photon absorption of benzene from ${}^1A_{1g}(S_0)$ to ${}^1B_{2u}(S_1)$, symmetry arguments indicate that the zero-th order electronic transition moment vanishes¹¹⁻¹³ or in other words, that the Condon approximation fails. Herzberg and Teller showed¹⁴ that the electronic transition moment μ is then induced by nuclear motions. For benzene, symmetry requires¹¹ that the leading order contributions to the dipole operator transform as E_{2g} . The sum in eq 2.15 is therefore restricted to the normal modes containing this symmetry. The induced transition moments appearing in Table 1 were taken from the $CNDO/S - CI$ computations of Ziegler and Albrecht¹⁵.

IV. Results

A. Benzene. Using the harmonic force field and dipole transition moments given in the previous section (see Table 1) we computed the absorption spectrum for benzene at $T = 300$ K and compared it with the experimental result¹⁶, as shown in Figure 1. The theoretical spectrum is computed with a pulse

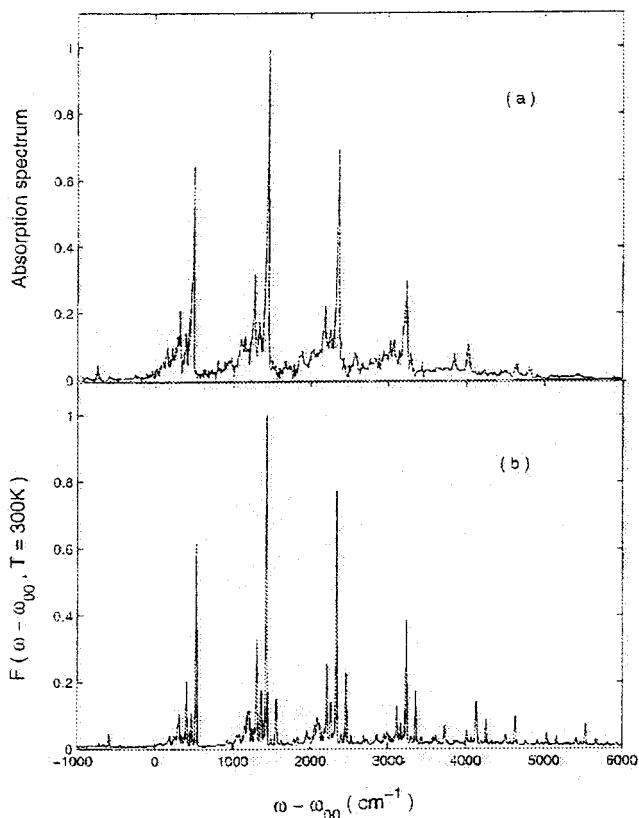


Figure 1. ${}^1B_{2u}(S_1) \leftarrow {}^1A_{1g}(S_0)$ absorption spectrum of benzene. Panel (a) shows the room temperature experimental spectrum of benzene vapor¹⁶. Panel (b) gives the $T = 300$ K theoretical spectrum, computed with eq 2.2 and a pulse duration of 1.0 psec.

duration of 1.0 ps. As may be seen from the figure the agreement between theory and experiment is very good, demonstrating that the ab initio force field and dipole transition strengths of the previous section provide a good description of the molecule. The strong peak around 500 cm^{-1} corresponds to the E_{2g} normal mode whose frequency is 529 cm^{-1} .

The average energy in the excited state (computed using eq 2.4) as a function of laser excitation frequency is shown for

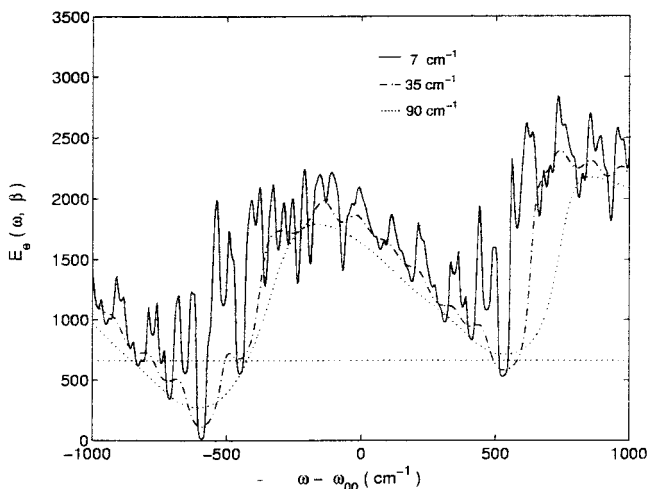


Figure 2. Average energy in the excited state is plotted as a function of excitation frequency for different pulse widths. The horizontal dotted lines denotes the thermal average energy at 300 K.

three different pulse widths in Figure 2. One notes that for a narrow pulse ($\Delta\omega = 7 \text{ cm}^{-1}$), the average energy is sensitive to the laser frequency, and it becomes less so as the pulse width is increased. The low average energy found around 500 cm^{-1} to the blue corresponds to a transition from the ground vibrational state of the E_{2g} mode in S_0 with frequency of 592 cm^{-1} to the first excited vibrational state in S_1 whose frequency is 529 cm^{-1} . Although this transition adds energy to the mode, the overlaps of the other modes are sufficiently weak so that there is a depopulation of the other modes and overall the average energy of the molecule in the excited state is slightly lowered. The low average energy found around 600 cm^{-1} to the red, corresponds to a transition from the first excited vibrational state of the E_{2g} mode in S_0 with frequency of 592 cm^{-1} to the ground vibrational state in S_1 whose frequency is 529 cm^{-1} . Here, it is this depletion of the population in the first excited vibrational state of the normal mode which significantly lowers the overall average energy.

One may translate the average energy in the excited state into an effective temperature by noting that the average energy for a thermal collection of harmonic oscillators at temperature T is ($\beta = 1/k_B T$)

$$\langle E \rangle_{\hbar(\beta)} = \sum_{j=1}^N \frac{\hbar\omega_j}{2} \coth\left(\frac{\hbar\beta\omega_j}{2}\right) \quad (4.1)$$

Given the harmonic frequencies in the S_1 state and the average energy as computed from eq 2.4 one can use eq 4.1 to find that temperature T_e , for which the canonical average energy equals the computed average energy. With this definition, we plot in Figure 3 the temperature T_e in the excited state as a function of laser excitation frequency. One notes that even for a relatively large pulse width ($\Delta\omega = 90 \text{ cm}^{-1}$) significant cooling is found to the red of the ω_{00} transition frequency. For the narrowest pulse studied ($\Delta\omega = 7 \text{ cm}^{-1}$), the population at the transition frequency of -592 cm^{-1} is almost exclusively in the ground vibrational state and the effective temperature is lowered to 73 K. Cooling is not as important in the transition to the blue and disappears completely for large pulse widths.

One may of course question whether the temperature assigned to the excited state has any physical meaning, since, the nascent energy distribution in the excited state is not canonical. In Figure 4, we plot the nascent vibrational energy distribution (smoothed with a Gaussian whose width is 100 cm^{-1} , computed using eq

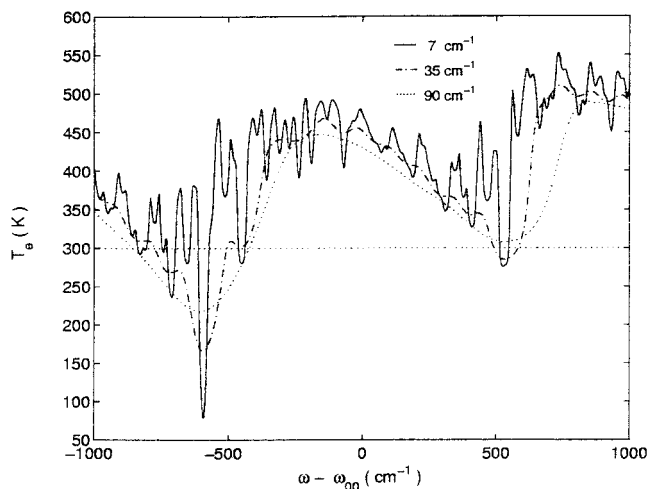


Figure 3. Effective vibrational temperature in the excited electronic state, defined by the average energy, plotted as a function of excitation frequency, for three different pulse widths. The horizontal dotted line denotes the temperature (300 K) of the ground electronic state.

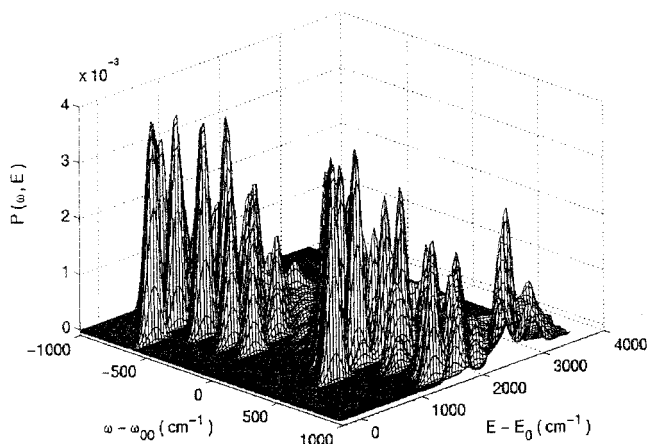


Figure 4. Nascent vibrational energy distribution in the excited state of benzene as a function of energy and excitation frequency. The resolution of the plots is $\Delta\omega = 7 \text{ cm}^{-1}$, $\Delta E = 100 \text{ cm}^{-1}$. The negative energies found at -592 cm^{-1} are an artifact of the finite energy resolution of 100 cm^{-1} .

2.6) as a function of the excitation frequency. One notes that the distribution is structured. More importantly, at $\omega = -592, 529 \text{ cm}^{-1}$, one notes that the energy distribution is substantially colder than at neighboring frequencies.

A different perspective is shown in Figure 5, where we compare the exact nascent energy distribution (also smoothed with a Gaussian whose width is 100 cm^{-1}) at four different excitation frequencies $\omega - \omega_{00} = -592, 200, 529,$ and 1300 cm^{-1} with the canonical distribution at the effective temperature T_e as determined above. As may be discerned from the figure, although the nascent energy distribution is not canonical, the canonical distribution at the temperature T_e does capture the main qualitative effect. At the frequencies of $\omega - \omega_{00} = -592, 529 \text{ cm}^{-1}$, the nascent energy distribution is found at significantly lower energies than at the other excitation frequencies. It is therefore reasonable to describe this effect as cooling and to use the effective temperature T_e as a “good” qualitative measure of the extent of the cooling involved in the process.

B. C_6D_6 . The absorption spectrum for room-temperature deuterated benzene is presented in Figure 6. The larger mass of Deuterium leads to a higher density of states and a lower frequency separation between peaks. The average energy and the effective temperature (determined through eq 4.1) of the

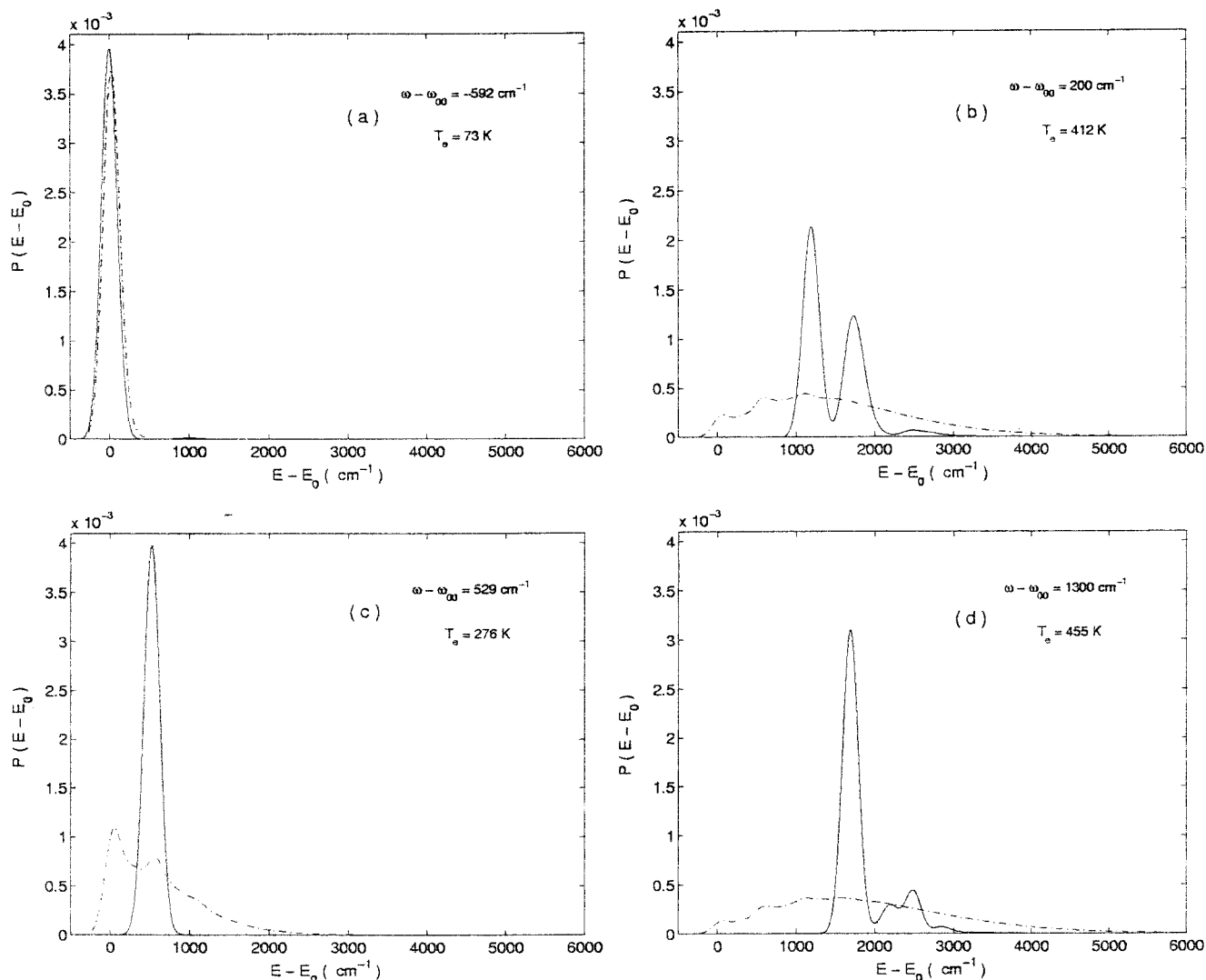


Figure 5. Cross-sections of the nascent vibrational energy distribution in the excited state of benzene. Panels a–d correspond to the excitation frequencies $\omega - \omega_{00} = -592, 200, 529, 1300 \text{ cm}^{-1}$. The solid lines show the exact nascent vibrational energy distributions, the dashed–dotted lines are the canonical distributions at the corresponding effective temperatures $T_e = 73, 412, 276, 455 \text{ K}$. Both distributions are smoothed with a Gaussian whose energy width is 100 cm^{-1} , this is the reason for the negative energy components.

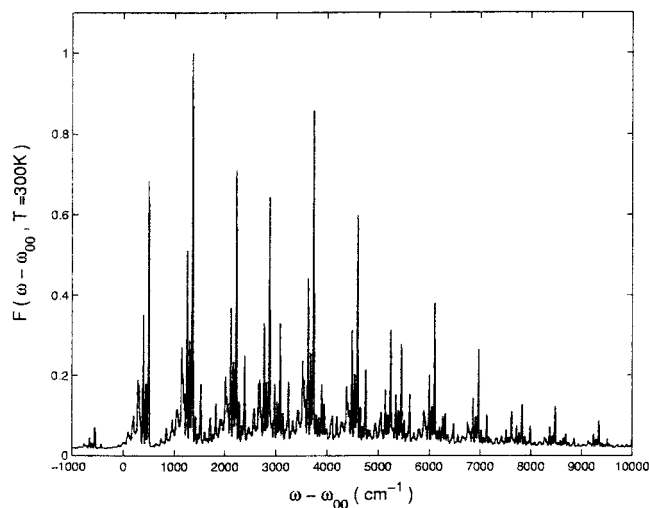


Figure 6. Calculated absorption spectrum of room temperature deuterated benzene. The pulse duration is 1.0 psec.

nascent vibrational energy distribution in the excited state (as defined in the previous subsection) is presented in Figure 7 as a function of laser frequency and for three different laser pulse

widths. Although the minimal temperature found for the deuterated species is somewhat higher than found for benzene (100 K), the range of frequencies which lead to cooling is larger. Thus for a broad pulse ($\Delta\omega = 90 \text{ cm}^{-1}$) the extent of cooling for deuterated benzene is roughly the same as for benzene. To the blue of the ω_{00} transition, one finds that deuterated benzene is colder than benzene itself, although even in the deuterated case, the cooling is not very large, reaching a minimum of 240 K. Even though energy is dumped into the excited state E_{2g} mode, the lack of sufficient overlap with the other modes causes cooling.

V. Discussion

Benzene is not the “ideal” molecule for the observation of cooling. Because the transition is symmetry disallowed, one must go a few hundred wavenumbers to the red or to the blue of the 0–0 transition before any significant absorption occurs. This implies that energy is typically dumped into the molecule rather than taken out of it. Even so, we found significant cooling in benzene both to the red and the blue, at the transition frequency corresponding to the lowest “large” absorption probability. Although we do not show it, if one goes beyond 1000 cm^{-1} to the red or to the blue of ω_{00} , only heating occurs,

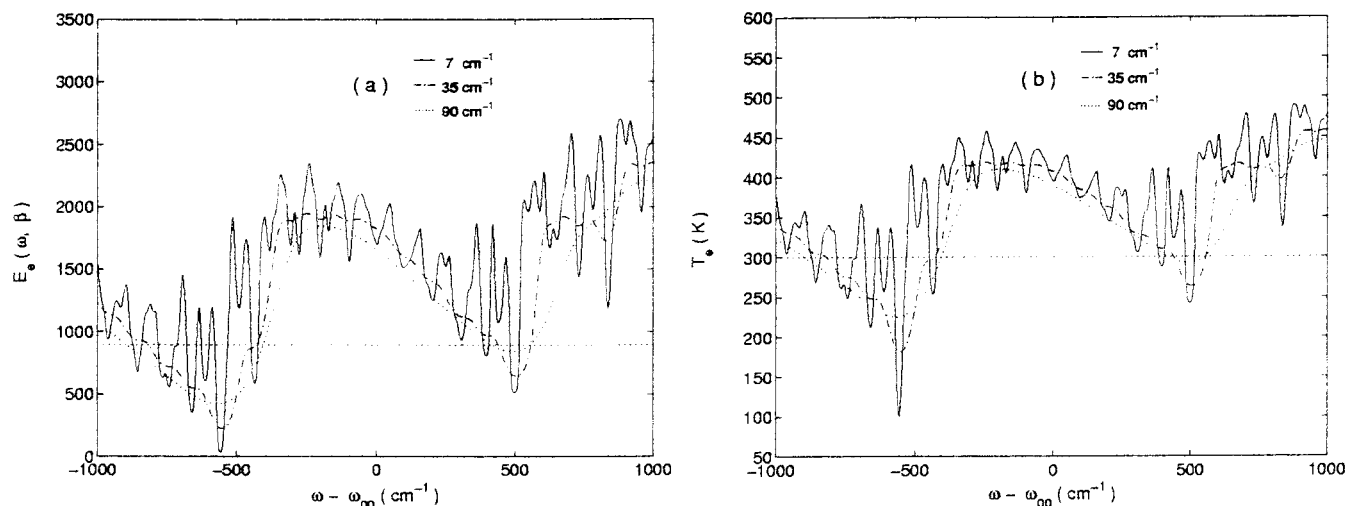


Figure 7. Average energy and the effective vibrational temperature in the excited electronic state of deuterated benzene (defined through the average energy) plotted as a function of excitation frequency for three different pulse widths. Panel a shows the average energy, and panel b shows the effective temperature. The horizontal dotted line in panel a denotes the average energy in the excited state at 300 K, whereas in panel b, it denotes the temperature (300 K) of the ground electronic state.

a large amount of energy is being transferred directly to the molecule and the frequency mismatch is not sufficient for cooling.

The extent of cooling depends on the width ($\Delta\omega$) of the excitation pulse. When the pulse is narrow, cooling is extensive, but limited to a narrow excitation frequency bandwidth. As the pulse becomes broader, the temperature increases, but cooling is observed over a rather large range of excitation frequencies. The selectivity of the excitation process is reduced as the width of the pulse is increased.

For a pulse whose width is 7 cm^{-1} or less, the average energy dumped into the excited state is a rather sensitive function of the excitation frequency. Changing the excitation frequency by 50 cm^{-1} can cause an average energy change of up to 2000 cm^{-1} . It has long been a dream of chemical physicists to induce mode dependent chemistry. Usually, the mode dependence disappears due to intramolecular vibrational redistribution. In benzene, we find that the average energy deposited in the molecule is sensitive to the frequency of excitation. The present study indicates that perhaps there is hope for frequency dependent control of excited-state reactions due to this sensitivity.

We have seen that deuteration does not cause a significant change in the overall picture. Cooling is found also for the deuterated case, over a range of a few hundred cm^{-1} in the photoexcitation frequency. Future studies on naphthalene and stilbene should shed further light on the chemistry of cooling of polyatomics by photoexcitation.

Finally, the study presented here is based on a harmonic model. At room temperature, for a molecule such as benzene whose lowest frequency is $\sim 1.8 k_B T$, one expects the harmonic approximation to be reasonable. The ab initio harmonic model

agrees well with the measured thermal absorption spectrum. It does remain though a challenge for future work to understand how anharmonicity and mode mixing affects the transition probabilities and thus the average energy dumped into the molecule.

Acknowledgment. We thank Dr. Y. Plimak for his help. This work was supported by a grant of the Israel Science Foundation and the Jubiläumsfonds der Oesterreichischen Nationalbank.

References and Notes

- (1) Beddard, G. S.; Fleming, G. R.; Gijzeman, O. L. J.; Porter, G. *Proc. R. Soc. London A* **1974**, *340*, 519.
- (2) Gershinsky, G.; Pollak, E. *J. Chem. Phys.* **1997**, *107*, 812.
- (3) Wadi, H.; Pollak, E. *J. Chem. Phys.* **1999**, *110*, 11890.
- (4) Swiderek, P.; Hohlneicher, G.; Maluendes, S. A.; Dupuis, M. *J. Chem. Phys.* **1993**, *98*, 974.
- (5) Duschinskii, F. *Acta Physicim. URSS* **1937**, *7*, 551.
- (6) Orlandi, G.; Palmieri, P.; Tarroni, R.; Zerbetto, F.; Zgierski, M. *Z. J. Chem. Phys.* **1994**, *100*, 2458.
- (7) Yan, Y. J.; Mukamel, S. *J. Chem. Phys.* **1986**, *85*, 5908.
- (8) Pulay, P.; Fogarasi, G.; Boggs, J. E. *J. Chem. Phys.* **1981**, *74*, 3999.
- (9) Wilson, E. B. Jr.; Decius, J. C.; Cross, P. C. *Molecular Vibrations*; McGraw-Hill: New York, 1955.
- (10) Miyazawa, T. *J. Chem. Phys.* **1958**, *29*, 246.
- (11) Atkinson, G. H.; Parmenter, C. S., *J. Mol. Spectrosc.* **1978**, *73*, 31.
- (12) Stephenson, T. A.; Radloff, P. L.; Rice, S. A. *J. Chem. Phys.* **1984**, *81*, 1060.
- (13) Page, R. H.; Shen, Y. R.; Lee, Y. T. *J. Chem. Phys.* **1988**, *88*, 5362.
- (14) Herzberg, G.; Teller, E. *Z. Phys. Chem. Abt. B* **1933**, *21*, 410.
- (15) Ziegler, L.; Albrecht, A. C. *J. Chem. Phys.* **1974**, *60*, 3558.
- (16) Pantos, E.; Philis, J.; Bolovinos, A. *J. Mol. Spectrosc.* **1978**, *72*, 36.
- (17) Callomon, J. H.; Dunn, T. M.; Mills, I. M. *Philos. Trans. (Royal Society, London) Ser. A* **1966**, *259*, 499.